Case Studies in Construction Materials 22 (2025) e04629

Contents lists available at ScienceDirect

Case Studies in Construction Materials

journal homepage: www.elsevier.com/locate/cscm

A novel self-curing active cold patch asphalt mixture: Performance evaluation and mechanism analysis

Xiong Xu [a,b], Kai Gong [a,b], Anand Sreeram [c], Zhifei Tan [d,e,*]

[a] School of Civil Engineering and Architecture, Wuhan Institute of Technology, Wuhan, China
[b] Hubei Provincial Engineering Research Center for Green Civil Engineering Materials and Structures, Wuhan Institute of Technology, Wuhan, China
[c] Nottingham Transportation Engineering Centre (NTEC), Faculty of Engineering, University of Nottingham, Nottingham, UK
[d] Department of Land Surveying and Geo-Informatics, The Hong Kong Polytechnic University, Hong Kong
[e] The Hong Kong Polytechnic University Shenzhen Research Institute, China

ARTICLE INFO

Keywords:
Cold patch asphalt mixtures (CPAMs)
Cold patch asphalt liquid (CPAL)
Self-curing reaction
Performance evaluation
Mechanism analysis

ABSTRACT

Cold patch asphalt mixtures (CPAMs) are increasingly favored for pothole repairs in asphalt pavements due to their environmental benefits and ease of construction. However, their low strength and durability have hindered broader application, necessitating the development of CPAMs with enhanced engineering performance. To address these challenges, this study proposes a novel self-curing active CPAM incorporating solvent naphtha (SN) as a diluent and polymerized methylene diphenyl diisocyanate (PMDI) as a polymer modifier. Various SN-to-PMDI ratios and SN-PMDI contents relative to virgin bitumen (VB) were evaluated to produce cold patch asphalt liquid (CPAL) and the corresponding CPAMs. Viscosity tests confirmed that SN effectively reduces VB viscosity, ensuring its workability. Specifically, adding 10 % SN reduced VB viscosity by approximately 30 %, while higher SN content (e.g., 30 %) significantly compromised mechanical performance. Mechanical evaluations, including Marshall stability, moisture susceptibility, crack resistance, freeze-thaw resistance, and rutting resistance, demonstrated that CPAM containing 20 % SN-PMDI with a 50:50 SN-to-PMDI ratio achieved excellent mechanical performance comparable to hot mix asphalt (HMA). Mechanism analysis through FTIR tests further revealed that PMDI reacts with atmospheric moisture, transforming isocyanate groups (-NCO) into carbamate groups (-NHCOO), and also interacts with hydroxyl groups on limestone aggregates, forming carbamate compounds, which contribute to a 20 % increase in strength development. Overall, this study introduces a novel approach for preparing high-performance CPAM, providing a promising solution for durable and efficient pothole repairs in practical engineering applications.

1. Introduction

After paving, asphalt pavements undergo various forms of deterioration due to environmental and traffic-induced effects [1,2]. Among these, potholes are one of the most common types of pavement distress. Potholes are bowl-shaped cavities of varying sizes that form when asphalt mixture is dislodged from the pavement surface [3,4]. They typically result from the degradation of the adhesion and cohesion properties of the asphalt mixture, particularly under the combined effects of water infiltration and traffic loads [5,6]. The

* Corresponding author at: Department of Land Surveying and Geo-Informatics, The Hong Kong Polytechnic University, Hong Kong.
E-mail address: zhi-fei.tan@connect.polyu.hk (Z. Tan).

https://doi.org/10.1016/j.cscm.2025.e04629
Received 31 December 2024; Received in revised form 1 March 2025; Accepted 5 April 2025
Available online 11 April 2025
2214-5095/© 2025 The Author(s). Published by Elsevier Ltd. This is an open access article under the CC BY-NC-ND license (http://creativecommons.org/licenses/by-nc-nd/4.0/).

formation of potholes accelerates pavement degradation and poses significant risks to driving safety [7,8]. Therefore, timely and effective pothole repair is essential to extend pavement lifespan and ensure road safety.

Hot mix asphalt (HMA) has traditionally been the preferred material for pothole repair [9–11]. While HMA repairs can restore pavement to its original performance, this method requires specialized heating and compaction equipment, making timely repairs, particularly in cold weather, challenging [12–14]. Additionally, producing small quantities of HMA for long-distance repairs is often impractical, limiting maintenance efficiency [15–17]. Recently, cold patch asphalt mixtures (CPAMs) have emerged as a viable alternative for pothole repairs. Unlike HMA, CPAMs use diluents to reduce the viscosity of the asphalt binder, enabling paving at ambient temperatures without heating. This offers significant advantages in terms of ease of construction and environmental sustainability [18–21]. However, it is important to note that CPAM differs from cold-mixed asphalt mixtures, which are made with emulsified asphalt and do not require heating during mixing and paving. In contrast, CPAMs still require heating during the mixing process (typically between 80°C and 100°C) to ensure proper workability [22,23]. While diluents improve workability at lower temperatures, they can reduce the cohesion of the asphalt binder, compromising the mechanical properties of CPAMs. As a result, CPAMs typically underperform compared to HMA, leading to reduced durability of repaired potholes [24–26] and diminished performance over time [27,28]. Therefore, despite the clear benefits of CPAM, enhancing its strength and durability remains a critical challenge.

The mechanical performance of CPAM largely depends on cold patch asphalt liquid (CPAL), which acts as the binder material in CPAM. Typically, CPAL consists of bitumen, diluents, and polymer modifiers [29–31]. Diluents reduce the viscosity of bitumen, enabling paving without heating, while polymer modifiers enhance the mechanical performance of CPAMs. Common diluents include petroleum-derived naphthas such as diesel, gasoline, and white naphtha [32,33]. Polymer modifiers like SBS, SBR, and epoxy resins are frequently used to improve CPAM's performance [34]. Additionally, additives such as water-resistance agents, rubber powders, fillers, and fibers have been incorporated into CPAM to improve its water resistance and rutting resistance [35–37]. However, the diluents and additives commonly used in CPAL often pose environmental concerns and incur high costs. Therefore, developing more environmentally friendly and cost-effective CPALs is imperative.

Solvent naphtha (SN), primarily derived from oil or natural gas, is a promising alternative diluent. It is a mixture of hydrocarbon compounds [38,39] with strong solvency, low cost, safety, and environmental benefits, making it widely used in industries such as chemical production, cleaning, and paint dissolution [40]. Similarly, polymerized methylene diphenyl diisocyanate (PMDI) is a potential polymer modifier for CPAL to enhance CPAM performance. PMDI improves water resistance and chemical corrosion resistance, reducing the damage caused by moisture and chemical exposure. When added in appropriate amounts and uniformly mixed, PMDI ensures effective reinforcement of CPAM. Zhang et al. [41] analyzed the chemical reaction mechanisms of polyurethane-modified asphalt (PUMA), highlighting PMDI's high reactivity, which enables nucleophilic addition reactions with active hydrogen-containing compounds such as alcohols, amines, and water. Cao et al. [42] demonstrated that the benzene ring structure of PMDI enhances the high-temperature rutting resistance of recycled SBS-modified asphalt. Li et al. [43] studied asphalt modified with polyurethane precursors, reporting good compatibility with pure asphalt. Zhang et al. [44] further showed that combining waste rubber powder with polyurethane significantly improved CPAL properties, outperforming single-modified CPAL. However, the

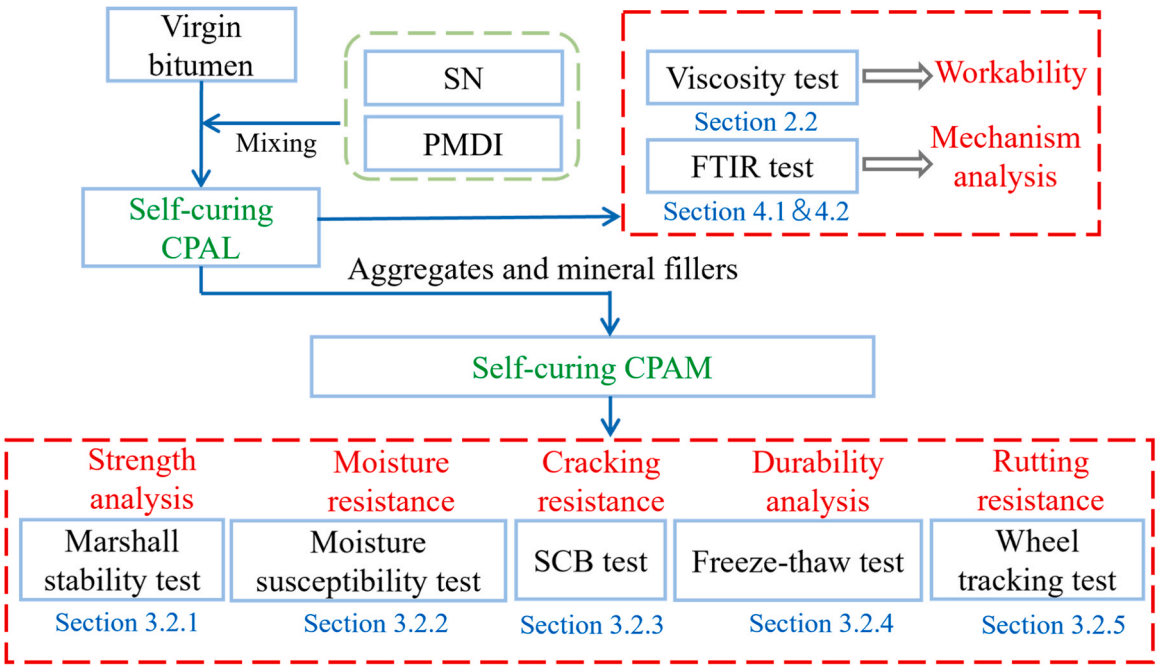

Fig. 1. Overview of this study.

application of SN and PMDI in CPAL remains underexplored.

To address this research gap, this study aims to develop a self-curing active CPAM. As illustrated in Fig. 1, SN and PMDI are proposed as the diluent and polymer modifier, respectively, to produce active CPAL. This active CPAL is then mixed with aggregates to prepare active CPAM. The fluidity of the active CPAL is evaluated through viscosity tests, while the engineering performance of the corresponding CPAM, including strength, moisture resistance, cracking resistance, durability, and rutting resistance, is assessed using Marshall stability tests, moisture susceptibility tests, semi-circular bend (SCB) tests, freeze-thaw tests, and rutting tests. Additionally, the curing mechanism of the active PMDI is investigated through Fourier-transform infrared spectroscopy (FTIR) analysis. The findings of this study are expected to advance both future research and practical applications of CPAM.

2. Cold patch asphalt liquid (CPAL) design and evaluation

2.1. CPAL design

In road engineering, binders such as virgin asphalt, emulsified asphalt, and polymer-modified asphalt are used to bond aggregates like sand and gravel. Their properties significantly influence the performance of the resulting mixture. For the CPAM investigated in this study, CPAL serves as the binder material. To prepare the CPAL, virgin bitumen (VB) with a penetration of 70 (Pen 70) was used in this study. It was supplied by Hanyang Municipal Engineering Co., Ltd., Hubei Province, China. The technical properties of the bitumen are summarized in Table 1.

To adjust the viscosity and workability of CPAL for paving applications, solvent naphtha (SN)—a petroleum-based diluent—was utilized. Unlike conventional petroleum-based diluents, SN offers superior solubility, lower cost, better safety, and environmental compatibility. The morphology and composition of SN are depicted in Fig. 2, while its physical properties are listed in Table 2.

Polymeric methylene diphenyl diisocyanate (PMDI) was employed as the polymer modifier due to its environmental benefits, economic viability, and excellent mechanical performance [45]. Fig. 3(a) and (b) illustrate the morphology and molecular structure of PMDI, while its physical properties are provided in Table 3.

As shown in Table 4, four SN-to-PMDI ratios (labeled as four groups) and five mass percentages of the SN-PMDI mix to VB (ranging from 5 % to 25 %) were considered to prepare CPAL. Fig. 4 outlines the preparation process. The VB was heated to 135 °C. Then, diluents and additives with varying mass ratios were added, followed by stirring for 30 min until the mix was homogeneous. The obtained CPALs are used to prepare CPAM. In the following, the CPALs and corresponding CPAMs were labeled using the format: Percent%(SN:PMDI)/VB. For example, 5 % (75SN:25PMDI)/VB indicates that CPAL with an SN-to-PMDI ratio of 75:25 was added at 5 % by mass relative to VB.

2.2. Viscosity evaluation of CPAL

Proper viscosity of CPAL is essential to ensure sufficient workability during the mixing and compaction of CPAMs [46]. The viscosity of CPAL is significantly influenced by the adding percentage of SN-PMDI into VB and SN to PMDI ratio. However, no standardized method currently exists for testing CPAL viscosity. To address this limitation, the Brookfield viscosity test was employed in this study to evaluate CPAL fluidity, following recommendations from previous research. The mixing temperature for CPAM preparation was set at 80°C. According to AASHTO M320, the viscosity of modified asphalt should range between 1000–3000 mPa·s at 80°C. Consequently, CPAL viscosity within this range was established as the workability criterion for evaluation.

Fig. 5 illustrates the measured viscosities of the prepared CPAL samples. Fig. 5(a) to (d) present viscosity trends for four groups of CPALs with SN:PMDI ratios decreasing from 100:0, 75:25, 50:50, to 25:75, respectively. It can be observed that as the SN content decreases, the viscosity of CPAL increases significantly, regardless of the percentage added into VB, demonstrating that SN effectively enhances fluidity. The influence of SN is particularly evident in Fig. 5(a), which represents 100SN:0PMDI, where the absence of PMDI isolates the effect of SN as a diluent. Increasing the SN content from 5 % to 10 % reduces the viscosity from 2005 mPa·s to 1180 mPa·s, nearly halving it. However, further increasing SN content from 15 % to 25 % produces only marginal reductions in viscosity, suggesting that an SN concentration above 15 % has a diminishing effect on fluidity improvement. This behavior may be attributed to the saturation of SN within the asphalt, where additional SN no longer integrates effectively but remains suspended, limiting further viscosity reduction.

Based on the viscosity requirements specified in AASHTO M320, the formulations that meet the workability criteria include 5–10 % (100SN:0PMDI)/VB, 5–20 % (75SN:25PMDI)/VB, 5–20 % (50SN:50PMDI)/VB, and 5–25 % (25SN:75PMDI)/VB. These results highlight the role of SN in improving fluidity and demonstrate that while PMDI increases viscosity due to enhanced structural rigidity, appropriate combinations of SN and PMDI can achieve the desired viscosity range for CPAL.

Table 1
Technical properties of virgin bitumen (VB).

Items	Results	Requirements	Specifications
Penetration at 25℃ (dmm)	67	60–80	ASTM D5
Softening point (℃)	48.1	$\geq$ 43	ASTM D36
Ductility at 15℃ (cm)	$>$ 100	$\geq$ 100	ASTM D113
Viscosity at 135℃ (Pa·s)	0.45	$\leq$ 3	AASHTO TP48

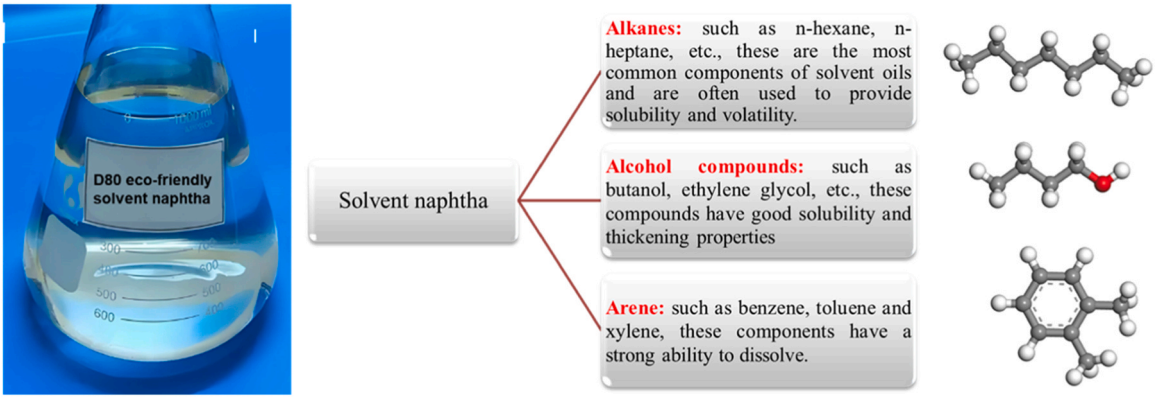

Fig. 2. Morphology and compositions of solvent naphtha (SN).

Table 2
Physical properties of solvent naphtha (SN).

Physical properties	Values
Density at 20℃ (g/cm^3)	0.805
Flash point (℃)	≥ 75
Boiling point (℃)	200–250
Viscosity at 25℃/40℃ (mPa·s)	2.16 /1.68
Proportion of Alkane/Alcohols/ Arene	40 %~70 %/10 %~40 %/5 %~20 %

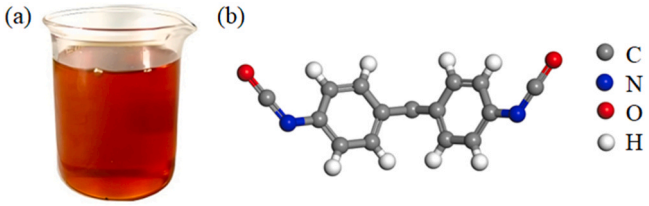

Fig. 3. Apparent morphology (a) and molecular structure (b) of PMDI.

Table 3
Physical properties of PMDI.

Physical parameter	Unit	Results
Appearance	/	Brown liquid
Viscosity (25℃)	mPa·s	100–250
Density (25℃)	g/cm^3	1.22
The proportion of -NCO	%	30.2–32.0

Table 4
Mix design for preparing CPAL.

Categories	SN:PMDI	Mass percentage of SN-PMDI mix to VB
Group 1	100:0	5 %/10 %/15 %/20 %/25 %(100SN:0PMDI)/VB
Group 2	75:25	5 %/10 %/15 %/20 %/25 %(75SN:25PMDI)/VB
Group 3	50:50	5 %/10 %/15 %/20 %/25 %(50SN:50PMDI)/VB
Group 4	25:75	5 %/10 %/15 %/20 %/25 %(25SN:75PMDI)/VB

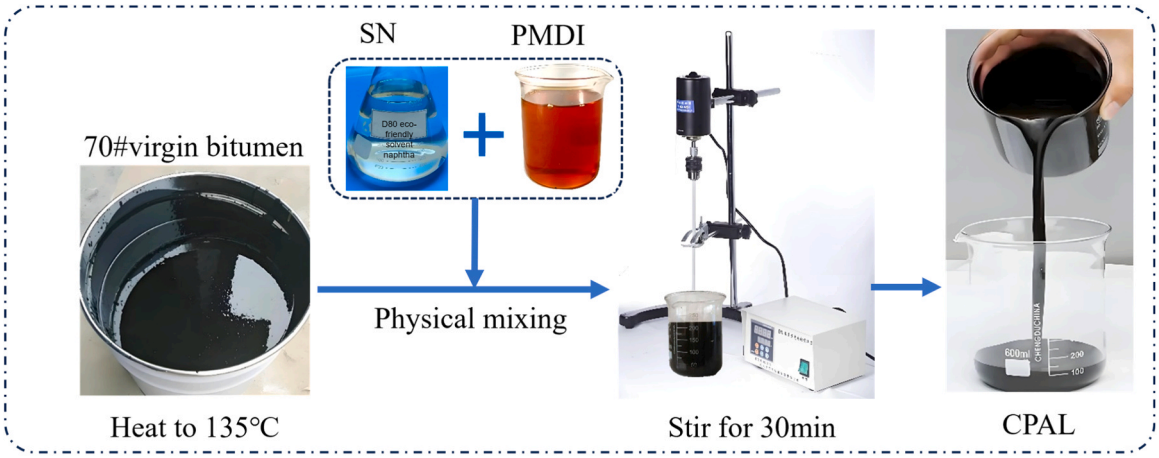

Fig. 4. Flowchart for preparation of CPAL.

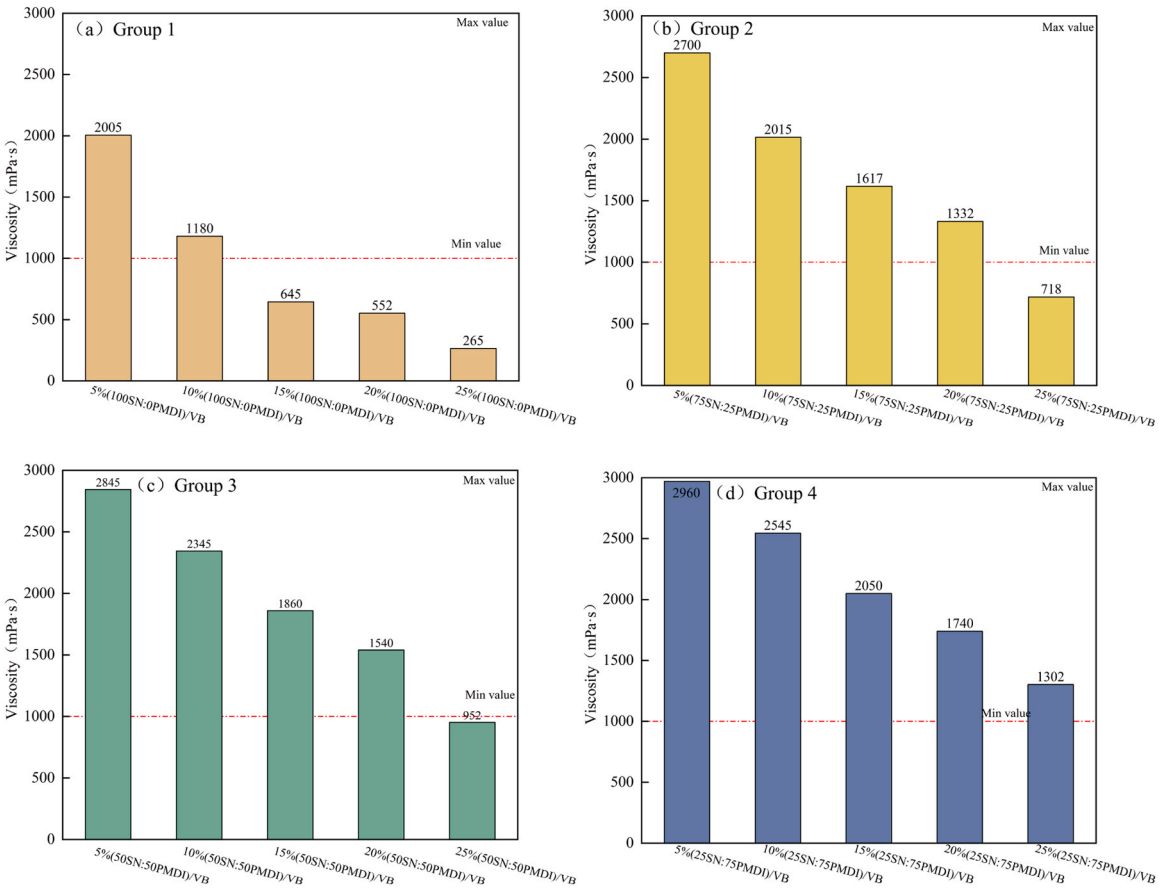

Fig. 5. Viscosity of CPALs at 80℃ (a) Group 1, (b) Group 2(c) Group 3 (d) Group 4.

3. Cold patch asphalt mixture (CPAM) design and evaluation

3.1. CPAM design

The coarse aggregate (2.36 mm~13.2 mm) and fine aggregate (0.075 mm~2.36 mm) used in this study were clean, dry, rough, and angular natural limestone. Table 5 summarizes the physical properties of natural limestone aggregates.

Table 5
Physical properties of natural limestone.

	Items	Unit	Results	Requirements
Coarse aggregate	Apparent density	g/cm^3	2.81	≥ 2.6
	Robustness	%	9	≤ 12
	Sand equivalent	%	42.4	≥ 30
	Stone crushing value	%	12.8	≤ 24
Fine aggregate	Apparent density	g/cm^3	2.72	≥ 2.5
	Robustness	%	8	≤ 12
	Sand equivalent	%	67	≥ 60
	Stone crushing value	%	8.45	≤ 24

Fig. 6 illustrates the process of preparing CPAM and repairing potholes. In this study, the gradation of a dense-graded asphalt mixture with a maximum nominal aggregate size (MNAS) of 13 mm (AC-13) was selected. To prepare the CPAM, the graded aggregates were preheated at 105 °C for 4 hours to remove moisture. The preheated aggregates were then transferred to a mixer maintained at 80°C and stirred for 90 seconds to ensure homogeneity. Subsequently, CPAL, preheated to 80°C, was added to the mixer and blended with the aggregates for an additional 90 seconds. Finally, mineral powder was gradually introduced, and mixing continued for another 90 seconds to ensure uniform distribution. Once cooled to ambient temperature, the prepared CPAM was ready for pothole filling and compaction.

It should be noted that the prepared CPAM may experience segregation after long-term storage. Therefore, it is recommended to re-stir the mixture thoroughly before paving. Once applied, CPAM gains strength through the evaporation of the diluent and the curing of PMDI under ambient conditions. Conventional CPAM typically achieves sufficient strength to open to traffic within 12 hours [47,48]. With the incorporation of PMDI, the self-curing CPAM proposed in this study requires less time to achieve the strength needed to open to traffic. For the test specimens prepared in this study, they were stored at ambient temperature and tested once they reached the specified curing time.

3.2. *Engineering performance evaluation of CPAM*

This section evaluates the engineering performance of the prepared CPAM through Marshall stability, moisture susceptibility, cracking resistance, freeze-thaw, and wheel-tracking tests.

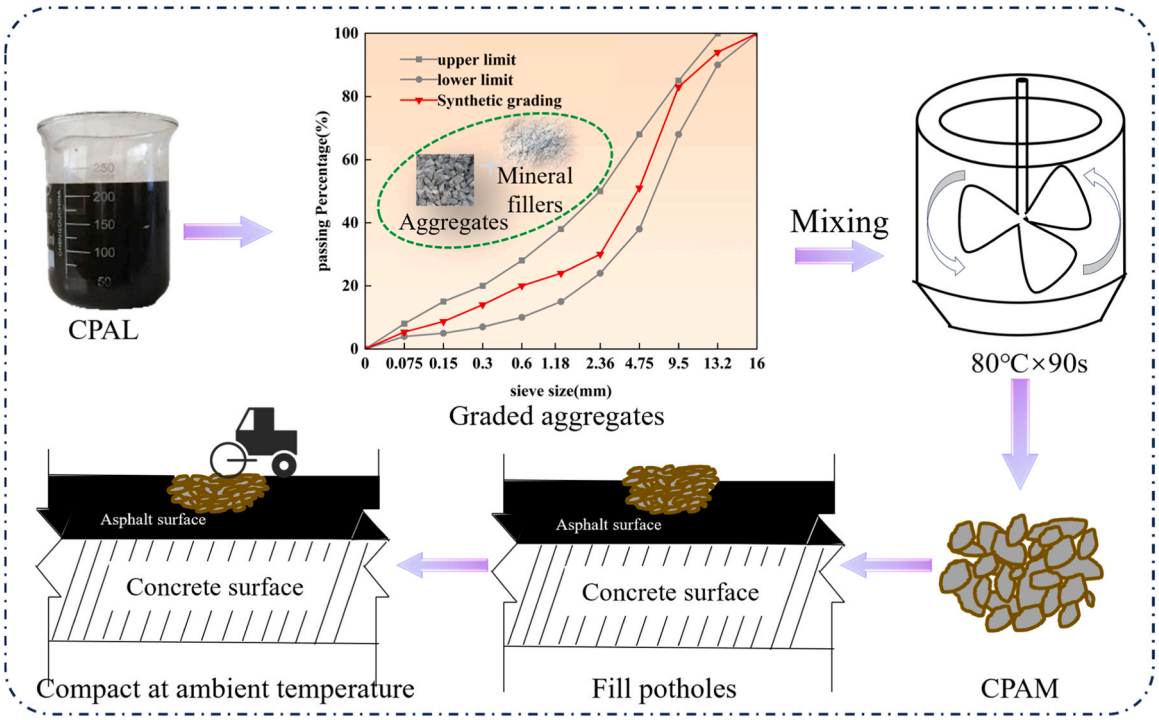

Fig. 6. CPAM preparation and pothole repair.

3.2.1. Marshall stability test

As SN evaporates and PMDI cures, the strength of CPAM gradually develops. Therefore, it is essential to assess both the initial stability and the formed stability after SN evaporation and PMDI curing. In this test, the initial stability was measured using Marshall samples stored at room temperature for 12 hours. For formed stability, the samples were first placed in an oven at 110 °C for 24 hours to accelerate strength development and then cooled at room temperature for 12 hours before testing.

The results of the initial and formed stability tests are presented in Fig. 7. Fig. 7(a) shows the stability results for CPAM with 100SN:0PMDI. Since this group contains no PMDI, it highlights the influence of SN alone. As the SN content increased from 5 % to 20 %, the initial and formed strengths of CPAM rose from 3.2 kN to 5.3 kN and 4.9–6.6 kN, respectively. This improvement can be attributed to SN's ability to enhance VB fluidity, thereby improving the bonding capability between aggregates. However, when the SN content increased further to 25 %, both the initial and formed stability exhibited a downward trend. This decline is primarily due to excessive SN acting as a diluent, which slows evaporation, resulting in reduced strength development during both the initial and final stages. Furthermore, across all SN contents, the formed stability was consistently higher than the initial stability, indicating that SN evaporation significantly contributes to strength improvement.

Fig. 7(b)–(d) display the Marshall stability results for CPAM samples with SN-PMDI contents ranging from 15 % to 25 %. It is evident that increasing the total SN-PMDI content from 15 % to 25 % has a negligible impact on stability. Among these, 20 % (50SN:50PMDI)/VB demonstrated the highest initial and formed stability. However, the SN:PMDI ratio was found to have a more pronounced effect on CPAM stability than the overall content percentage. Regardless of the added percentage, as the SN:PMDI ratio decreased from 100:0–25:75, the stability first increased, reaching a peak at 50:50, and then declined. This trend suggests that PMDI effectively promotes strength development, acting as a reinforcing agent. However, excessive PMDI content reduces CPAL fluidity, impeding uniform coating of the aggregates and ultimately weakening the structural integrity of the CPAM.

Overall, the optimal performance was achieved with a 50SN:50PMDI ratio, which balanced fluidity and strength development. Under the combined effects of SN evaporation and PMDI curing, the formed stability showed significant improvement compared to the initial stability, highlighting the contribution of these dual mechanisms to CPAM's strength enhancement.

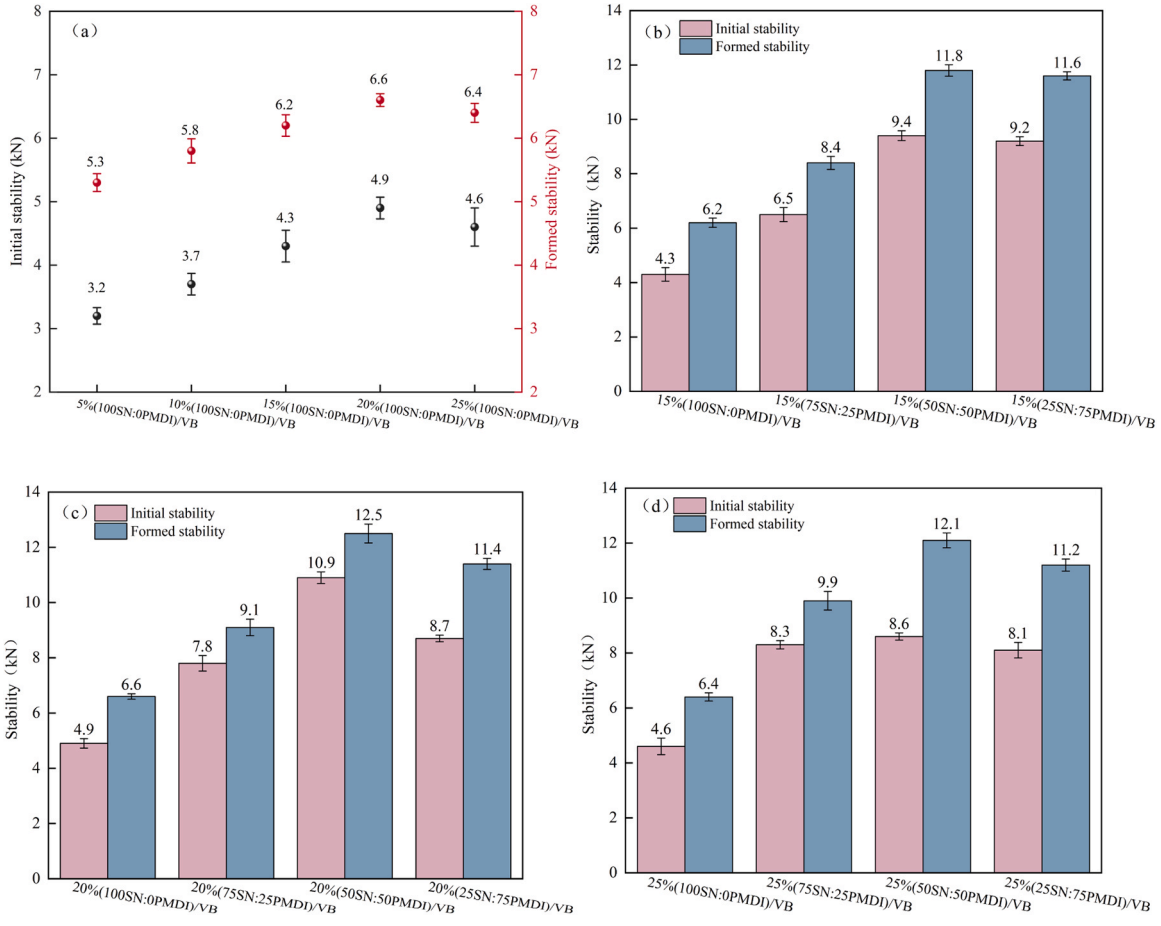

Fig. 7. Initial and formed stability: (a) Samples of 100SN:0PMDI, (b) Samples with 15 % SN-PMDI content, (c) Samples with 20 % SN-PMDI content, and (d) Samples with 25 % SN-PMDI content.

3.2.2. Moisture susceptibility test

To assess the moisture resistance of the prepared CPAMs, Marshall stability (MS) tests were conducted on samples subjected to water conditioning at 60 °C for 48 hours. Fig. 8 presents the Marshall stability values of the CPAM samples both before and after water conditioning. It is noteworthy that the specimens in Group 1 (100SN:0PMDI), containing only SN, exhibited significant water damage after conditioning. The compacted mixtures in this group became loose and disintegrated, rendering them unsuitable for further evaluation. Consequently, no results are shown in Fig. 8 for this group. This finding highlights the adverse impact of SN alone on moisture resistance, emphasizing the necessity of incorporating PMDI to improve durability.

Fig. 8(a)–(c) illustrate the stability results for CPAMs prepared with SN-PMDI contents ranging from 15 % to 25 %. The stability values increased as the SN-PMDI content rose from 15 % (Fig. 8a) to 20 % (Fig. 8b). However, when the content increased further to 25 % (Fig. 8c), only the sample with 75SN:25PMDI demonstrated improved strength, while the samples with 50SN:50PMDI and 25SN:75PMDI exhibited slight decreases in strength. These results suggest that 20 % SN-PMDI is the optimal content for CPAM, providing a balance between strength and moisture resistance. Among the tested SN:PMDI ratios (75:25, 50:50, and 25:75) at 20 % SN-PMDI, the 50SN:50PMDI formulation exhibited the highest stability both before and after conditioning. This superior performance can be attributed to the synergistic effects of SN and PMDI. Specifically, the 75SN:25PMDI formulation, with a high SN and low PMDI content, compromised the strength of the CPAM due to insufficient curing. Conversely, the 25SN:75PMDI formulation, with a lower SN content, reduced the workability of CPAL during mixing, leading to incomplete aggregate coating and diminished structural integrity.

To further evaluate the impact of water conditioning, the residual Marshall stability (RMS) was calculated, and the results are shown in Fig. 8(d). It is evident that the 20 %(50SN:50PMDI)/VB formulation demonstrated the highest RMS. Based on the 80 % minimum RMS requirement for asphalt mixtures, the following formulations satisfied the criterion: 20 %(50SN:50PMDI)/VB, 20 % (25SN:75PMDI)/VB and 25 %(50SN:50PMDI)/VB. These results underscore the importance of optimizing the SN:PMDI ratio and content to ensure moisture resistance and mechanical stability in CPAM formulations.

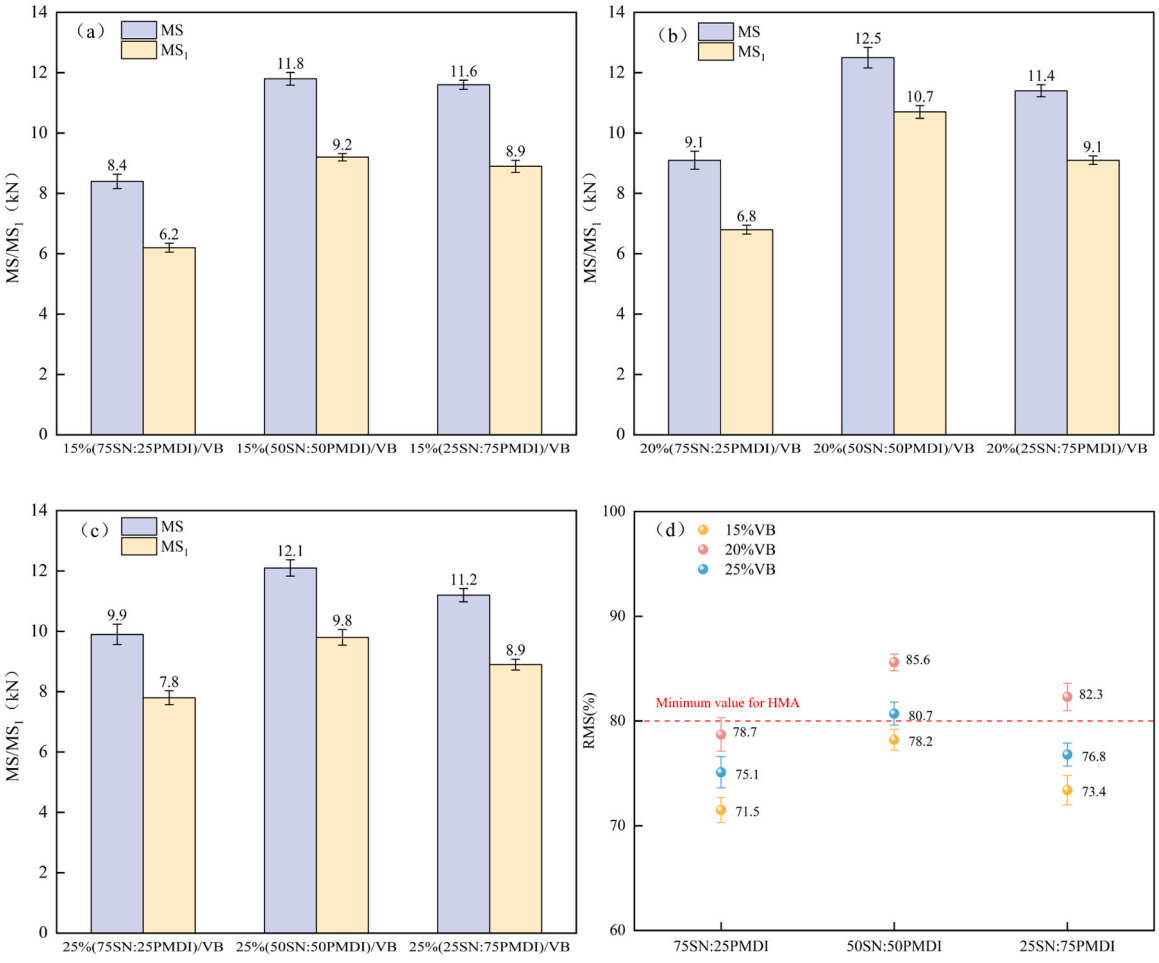

Fig. 8. Marshall stability (MS) before and after water conditioning: (a) Samples with 15 % SN-PMDI content, (b) Samples with 20 % SN-PMDI content, (c) Samples with 25 % SN-PMDI content and (d) Residue Marshall stability (RMS).

3.2.3. Crack resistance test

To evaluate the anti-cracking performance of the prepared CPAM, semi-circular bend (SCB) tests were conducted. The SCB test is one of the most commonly used methods for assessing the cracking resistance of asphalt mixtures. Based on the obtained load-displacement curve, the fracture energy (G_f) was calculated to evaluate the material's ability to resist crack propagation under stress.

Fig. 9(a) and (b) illustrate the peak load and calculated fracture energy for all tested CPAMs. It can be observed that the peak load and fracture energy exhibit similar trends with varying SN:PMDI ratios. Both the peak load and fracture energy increase as the SN:PMDI ratio changes from 100:0–50:50 but decrease as the ratio further increases to 25:75. This behavior can be attributed to the distinct roles of SN and PMDI. SN primarily improves the workability of CPAM during mixing, while PMDI enhances the strength of CPAM through its curing properties. An appropriate SN:PMDI ratio balances these effects, achieving optimal performance. From Fig. 9. it is evident that CPAM prepared with CPAL containing 20 % (50SN:50PMDI) exhibits the best anti-cracking performance, with a maximum peak load of 26.6 kN and a fracture energy of 10191 J/m^2.

3.2.4. Freeze-thaw test

The freeze-thaw test was conducted in accordance with ASTM D 5569 to assess the impact of freeze-thaw cycles on the mechanical performance of the prepared CPAM samples. Fig. 10 presents the indirect tensile strength (ITS) of the specimens before and after undergoing freeze-thaw conditioning. Fig. 10(a)–(c) illustrate the ITS results for CPAMs prepared with SN-PMDI contents ranging from 15 % to 25 %. Similar to the moisture susceptibility test results, an increase in SN-PMDI content initially enhances the ITS values, followed by a decline at higher contents, both before and after freeze-thaw conditioning. These findings indicate that a 20 % SN-PMDI content achieves an optimal balance between strength and freeze-thaw resistance.

Fig. 10(d) presents the tensile strength ratio (TSR), which quantifies the retained strength of samples after freeze-thaw conditioning. Based on the 85 % minimum TSR requirement for asphalt mixtures, six CPAM formulations meet the specified criteria: 15 ~25%(50SN:50PMDI)/VB, 20 %(25SN:75PMDI) and 15~20 %(25SN:75PMDI). These results underscore the robustness of the 50SN:50PMDI formulation, which demonstrates excellent performance under freeze-thaw conditions. Additionally, the 25SN:75PMDI formulations at lower content levels also exhibit adequate resistance to freeze-thaw damage, highlighting their potential suitability for regions subjected to severe temperature fluctuations.

3.2.5. Wheel tracking test

The rutting resistance of the prepared CPAM was evaluated using the wheel tracking test (WTT) in accordance with ASTM D6935. Based on the results obtained from the Marshall and freeze-thaw tests, rutting tests were conducted only on CPAM samples containing 20 % SN-PMDI added to VB. To simulate different climatic conditions, WTT was performed at 45°C and 60°C. The rut depth progression during testing is illustrated in Fig. 11. The development of rut depth can be classified into three distinct stages. In the initial compaction stage, which occurs within the first 20 minutes, the CPAM undergoes densification under the rolling wheel, resulting in reduced air voids. The second stage, between 20 and 45 minutes, is characterized by a flow process in which further reduction in air voids causes the asphalt matrix to be squeezed out of the CPAM under the applied wheel load, leading to significant deformation. In the final stage, from 45 to 60 minutes, continued loading induces aggregate rearrangement, particularly at the edges of the wheel path, where shear forces displace aggregates, resulting in additional deformation.

As shown in Fig. 11, regardless of temperature, the formulation 20 %(50SN:50PMDI)/VB exhibited the best rutting resistance, as evidenced by the slowest rate of rut depth increase. This was followed by 20 %(25SN:75PMDI)/VB, 20 %(75SN:25PMDI)/VB, and 20 %(100SN:0PMDI)/VB. A comparison between 20 %(50SN:50PMDI)/VB and 20 %(25SN:75PMDI)/VB reveals a significantly higher rut depth in the latter during the second and third stages, despite its higher PMDI content. This discrepancy can be attributed to two primary factors. Firstly, the lower SN content compromises the mixing effectiveness between CPAL and aggregates. Secondly, excessive PMDI may lead to residual uncured material within the CPAM, weakening the overall structure. Similarly, 20 %(75SN:25PMDI)/VB and 20 %(100SN:0PMDI)/VB exhibited considerably higher rut depths across all three stages, which can be attributed to their

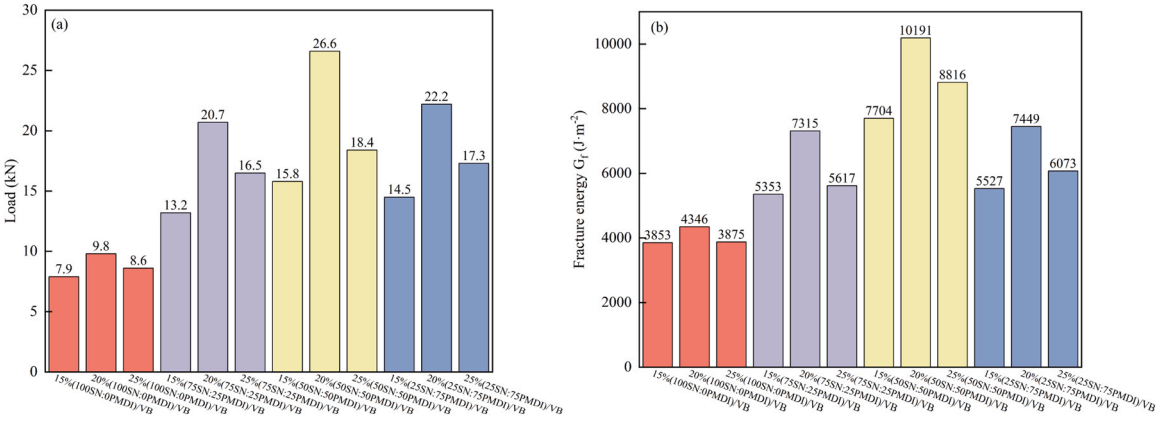

Fig. 9. SCB test results: (a)Peak load, (b) Fracture energy.

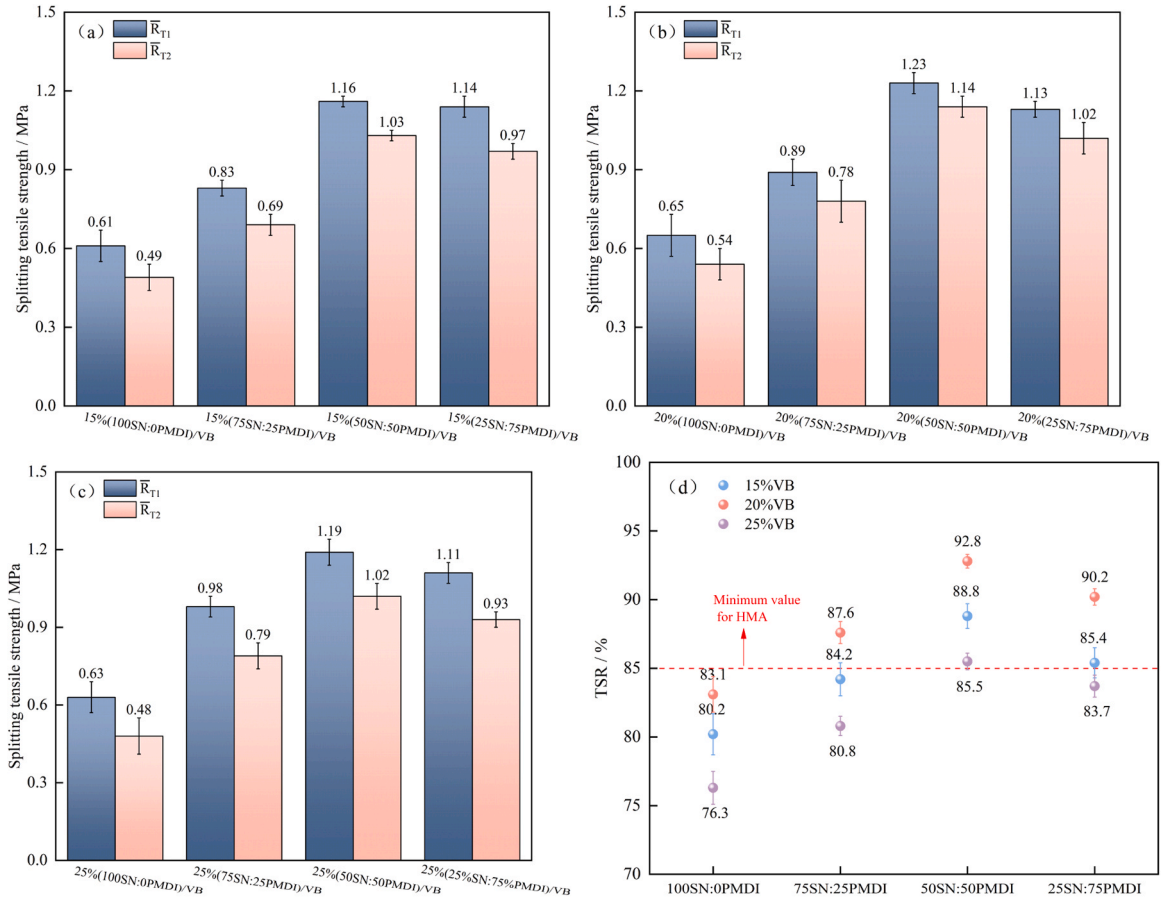

Fig. 10. ITS before and after freeze-thaw cycle: (a) Samples with 15 % SN-PMDI content, (b) Samples with 20 % SN-PMDI content, (c) Samples with 25 % SN-PMDI content and (d) Tensile strength ratio (TSR).

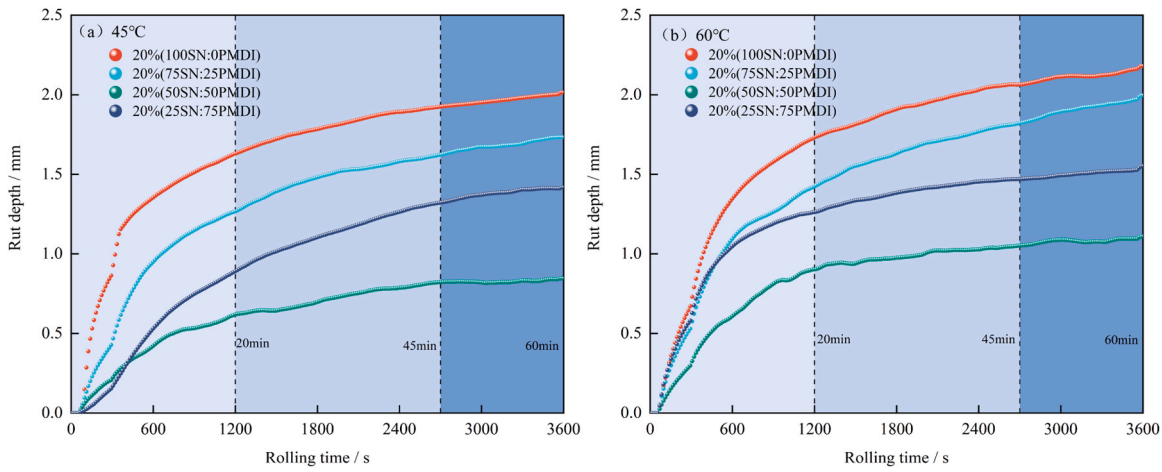

Fig. 11. Rut depth of CPAM: (a) 45℃; (b) 60 ° C.

excessively high SN content, resulting in a reduction in structural strength.

A comparison of rut depths at 45°C (Fig. 11a) and 60°C (Fig. 11b) further highlights the influence of temperature. For the formulation 100SN:0PMDI, rut depths at 45°C and 60°C were 1.96 mm and 2.28 mm, respectively, reflecting a difference of 0.32 mm. In contrast, the formulation 50SN:50PMDI exhibited rut depths of 0.92 mm and 1.11 mm, resulting in a much smaller increase of

0.19 mm. These results demonstrate that the addition of PMDI enhances the high-temperature deformation resistance of CPAM, making it less susceptible to temperature fluctuations.

The development of dynamic stability (DS) with curing time was further evaluated to assess the impact of curing on rutting resistance. The strength of CPAM increases over time as PMDI cures. DS values were measured after 0, 2, 4, 6, and 8 days of curing, and the results are presented in Fig. 12. As shown in the Fig. 12, DS increased rapidly during the first four days for all CPAM samples, indicating rapid strength development. After six days, the curves flattened, suggesting that the curing process of PMDI had largely stabilized. Consistent with the rut depth results, 20 %(50SN:50PMDI)/VB exhibited the highest DS values and the fastest rate of increase, followed by 20 %(25SN:75PMDI)/VB, 20 %(75SN:25PMDI)/VB, and 20 %(100SN:0PMDI)/VB.

The curing time required to meet the minimum DS requirements for asphalt mixtures was also analyzed. It was found that 20 %(50SN:50PMDI)/VB satisfied the minimum requirement after three days of curing. In comparison, 20 %(25SN:75PMDI)/VB and 20 %(75SN:25PMDI)/VB required four days of curing to meet the same standard. These findings underscore the importance of balancing SN and PMDI content in CPAM formulations to optimize rutting resistance and curing performance under varying temperature conditions. Furthermore, the rutting test results demonstrate that the mixture exhibits good rutting resistance once the diluent evaporates. As the diluent evaporates, the binder becomes thicker and more cohesive, enhancing the bond between the aggregates and the binder. The DS value after four days reached the standard value of HMA, indicating that the solvent is completely volatilized within this period. This results in a stronger bond between the aggregates and the binder, significantly improving the mixture's overall mechanical properties.

4. Mechanism analysis

4.1. Curing mechanism of CPAL with moisture in air through FTIR spectrum analysis

During the curing process of CPAM, the PMDI component in CPAL reacts with hydroxyl groups from moisture in the air. To investigate this mechanism, a Thermo Scientific Nicolet iS10 Fourier Transform Infrared (FTIR) Spectrometer was employed to analyze the functional group changes in CPAL. The attenuated total reflectance Fourier-transform infrared (ATR-FTIR) mode was used, scanning samples within the wavelength range of 4000 cm^{-1} to 400 cm^{-1} at a resolution of 4 cm^{-1} , with 32 scans performed for each test.

Fig. 13 displays the measured spectra for VB, 20 %(100SN:0PMDI)/VB, and 20 %(50SN:50PMDI)/VB at 0 days and 5 days of curing. VB and 20 %(100SN:0PMDI)/VB served as control groups to identify the characteristic peaks of VB and SN, respectively. The primary absorption peaks are summarized in Table 6. The peaks observed at 2957 cm^{-1} , 2920 cm^{-1} , and 2850 cm^{-1} correspond to the asymmetric and symmetric stretching vibrations of C–H bonds in methyl (-CH_3) and methylene (-CH_2-) groups within VB. Similarly, the peaks at 1453 cm^{-1} and 1375 cm^{-1} correspond to the bending vibrations of C–H bonds in -CH_2- and -CH_3 groups, respectively.

When comparing the spectrum of 20 %(100SN:0PMDI)/VB with VB, a distinct peak at 3668 cm^{-1} is observed, attributed to the alcohol (-OH) groups in SN molecules. For 20 %(50SN:50PMDI)/VB at 0 days, a new peak appears at 2269 cm^{-1} , associated with the stretching vibration of the isocyanate group (-N = C═O) in PMDI. Additionally, a sharp absorption peak at 1510 cm^{-1} corresponds to the bending vibration of the -NH group. After 5 days of exposure to air, the absorption peak of the isocyanate group (-NCO) at 2269 cm^{-1} diminishes, while new peaks emerge at 1653 cm^{-1} (amide I band) and 1308 cm^{-1} (amide III band), corresponding to the stretching vibrations of carbonyl (-C═O) groups in carbamate. Other notable peaks include 1230 cm^{-1} , attributed to the stretching of C–O bonds in carbamate, and 1070 cm^{-1} , related to the deformation vibration of aromatic C–H bonds. The characteristic peaks of -N = C═O, -C═O, and C–H indicate the consumption of isocyanate groups (-NCO) and the formation of carbamate groups (-NHCOO). These observations confirm that polymerization reactions occur within CPAL during curing.

To quantify the reaction extent of PMDI, the peak area ratios of the isocyanate group (-NCO) to the -CH bond were calculated, as shown in Fig. 13. On day 0, the ratio was 25 %, which reduced to 2 % after 5 days, indicating that the initial peak area of isocyanate groups was approximately 12.5 times larger than that after curing. This semi-quantitative analysis demonstrates that the majority of active PMDI's isocyanate groups were consumed within 5 days. These findings provide critical insights into the curing mechanism and efficiency of CPAL polymerization.

4.2. Reaction mechanism of active PMDI in CPAM

Based on the FTIR analysis presented in Section 4.1 and supporting literature in Introduction section, the curing mechanism of CPAM involves four primary chemical reactions, as illustrated in Fig. 13. In the first reaction, the isocyanate group (-N = C═O) in PMDI reacts with hydroxyl groups (-OH) from ambient moisture, generating amino groups (-NH_2) and releasing carbon dioxide (CO_2), as depicted in Fig. 14(i). This reaction leads to changes in the infrared bands, particularly the disappearance of the -N = C═O peak at 2269 cm^{-1} and the appearance of the -NH peak at 1510 cm^{-1} [49,50]. In the second reaction, the isocyanate group (-NCO) reacts with amino groups (-NH_2) to form carbamate groups (-NHCOO), as shown in Fig. 14(ii). This process results in the formation of rigid chain segments, contributing to structural strength. The third reaction involves the polymerization of intermediates formed in the previous steps, resulting in the development of rigid polymeric structures. Peaks at 1710 cm^{-1} , 1653 cm^{-1} , and 1308 cm^{-1} correspond to the stretching vibrations of carbonyl (-C═O) groups, while the peak at 1070 cm^{-1} is associated with aromatic C–H bonds, as illustrated in Fig. 14(iii). Finally, the fourth reaction occurs when the isocyanate group (-NCO) reacts with hydroxyl groups (-OH) to form ester compounds, particularly urea derivatives, as shown in Fig. 14(iv). Additionally, due to the abundance of alkaline hydroxyl groups in limestone aggregates, it can be inferred that these hydroxyl groups can also react with PMDI, forming carbamate groups that enhance the bonding and mechanical strength of CPAM [50–52].

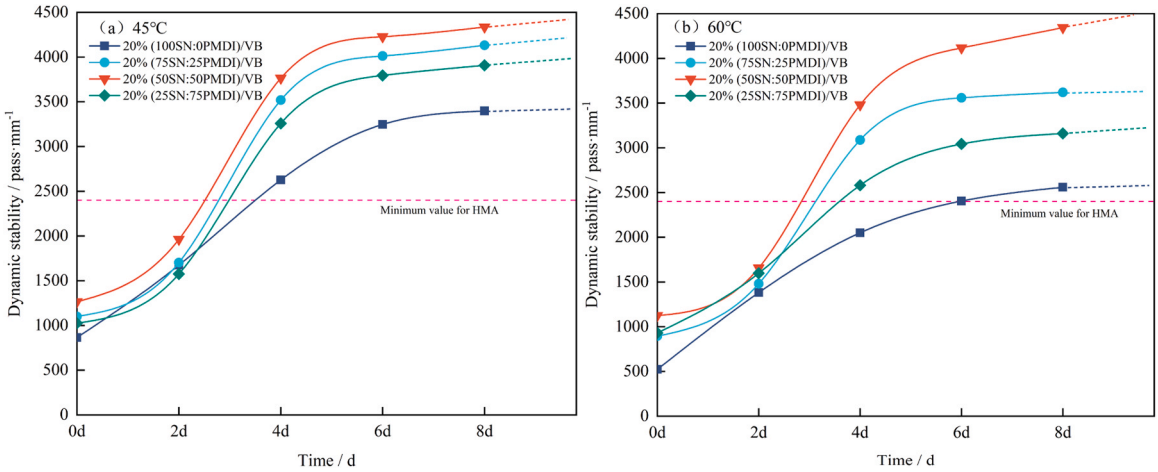

Fig. 12. Dynamic stability (DS) development with curing time (a) 45℃; (b) 60℃.

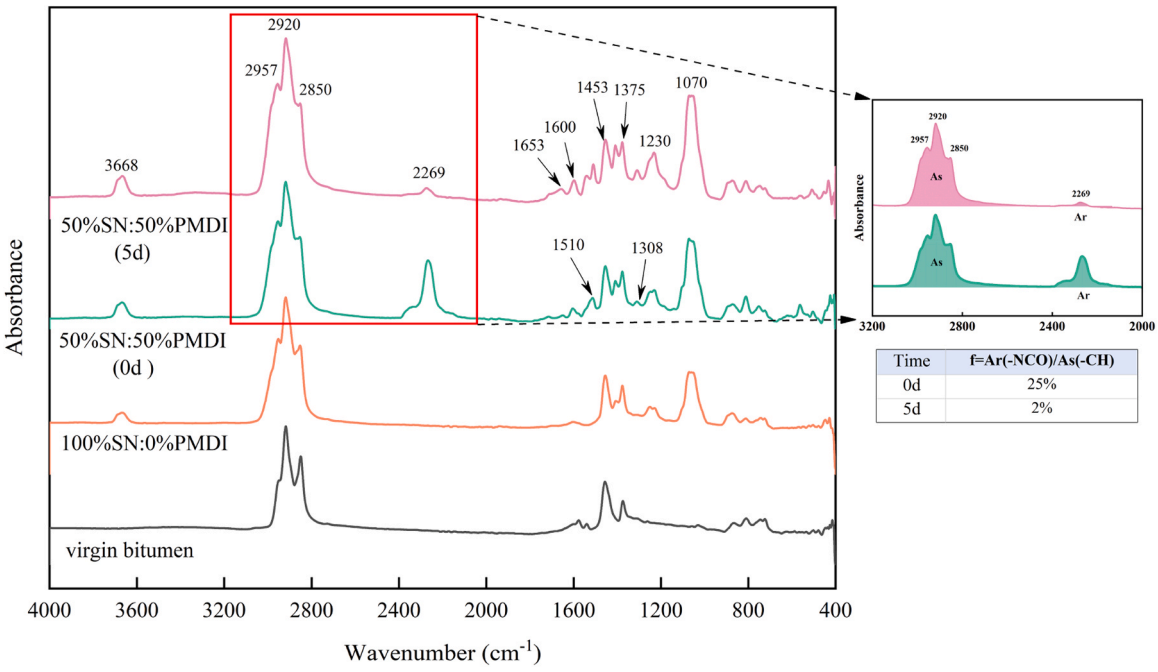

Fig. 13. ATR-FTIR spectra of asphalt CPAL.

Table 6
Description of the spectrum peak of asphalt CPAL.

Wavenumber(cm^{-1})	Attribution	Vibration type
3668	-OH	O-H stretching
2957,1375	$-CH_3$	C-H asymmetric and symmetric stretching
2920,2850,1453	$-CH_2-$	C-H asymmetric and symmetric stretching
2269	-N═C═O	Stretching vibration of double bond
1653,1308	-C═O	C═O stretching vibration (five-membered ring)
1600	C═C	C═C stretching
1510	-NH	-NH bending
1230, 1070	C-H	C-H stretching

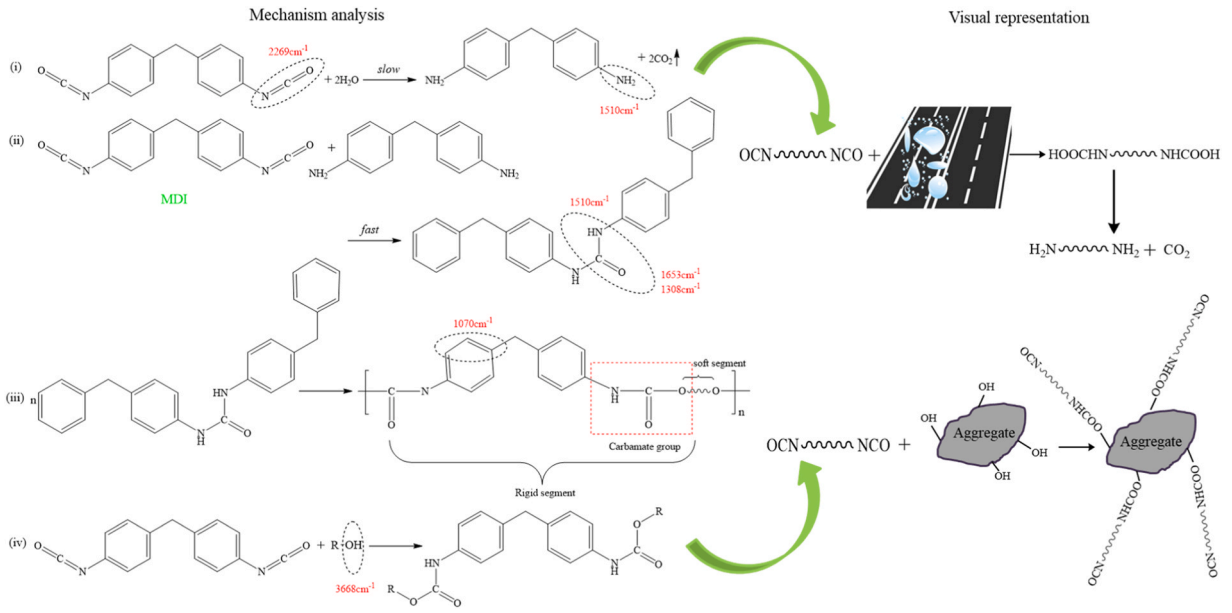

Fig. 14. Reaction mechanism analysis of active PMDI.

These chemical reactions collectively play a pivotal role in the curing and hardening process of CPAM, improving its mechanical performance and durability. The formation of carbamate groups and polymeric structures ensures effective bonding within the asphalt matrix, providing enhanced resistance to deformation and environmental degradation.

5. Conclusions

This study explored the use of solvent naphtha (SN) as a diluent and polymerized methylene diphenyl diisocyanate (PMDI) as a polymer modifier to develop a high-performance, reactive cold patch asphalt liquid (CPAL). The effects of varying SN-PMDI content and SN-to-PMDI ratios in virgin bitumen (VB) were systematically investigated. Based on the evaluation and mechanism analysis of CPAL and its corresponding cold patch asphalt mixture (CPAM), the following conclusions can be drawn:

- Viscosity evaluation on CPAL indicated that the addition of SN significantly reduces the viscosity of VB, enabling cold mixing. A concentration of 15 % SN relative to VB is sufficient to achieve the desired viscosity reduction for CPAM preparation. Increasing the SN content beyond this level offers no further viscosity reduction and may compromise the mechanical performance of CPAM.
- Mechanical testing demonstrated that the percentage of SN-PMDI and the SN-to-PMDI ratio significantly influence stability, water resistance, crack resistance, freeze-thaw durability, and rutting resistance. CPAM with 20 % SN-PMDI and a 50:50 SN-to-PMDI ratio—denoted as 20 %(50SN:50PMDI)/VB—exhibited the best overall mechanical performance.
- FTIR analysis confirmed that PMDI reacts with atmospheric moisture, achieving a high reaction rate within five days. The transformation of isocyanate groups (-NCO) into carbamate groups (-NHCOO) was validated through the disappearance of the -NCO peak and the emergence of -C═O peaks. In CPAM, PMDI further reacts with hydroxyl groups on the surface of limestone aggregates, forming carbamate groups. These chemical reactions are essential for strength development in CPAM.
- FTIR analysis confirmed that PMDI reacts with atmospheric moisture, achieving a high reaction rate within five days. The transformation of isocyanate groups (-NCO) into carbamate groups (-NHCOO) was validated through the disappearance of the -NCO peak and the emergence of -C═O peaks. In CPAM, PMDI further reacts with hydroxyl groups on the surface of limestone aggregates, forming carbamate groups. These chemical reactions are essential for strength development in CPAM.

In conclusion, this study proposes a novel technical approach for preparing CPAM with excellent mechanical performance, offering promising applications for pothole repairs in engineering practice. However, further research is recommended to investigate the long-term performance and micro-mechanisms of strength development in the proposed CPAM. Currently, the material has been applied to small-scale pavement repairs and will be scaled up for practical pavement maintenance projects. Its long-term performance under field conditions, including fatigue resistance, aging behavior, and durability, will be evaluated. Additionally, TG/DSC tests will be conducted to further elucidate the micro-mechanisms underlying the strength development of CPAM.

CRediT authorship contribution statement

Xiong Xu: Writing – review & editing, Supervision, Methodology, Conceptualization. **Kai Gong:** Writing – original draft,

Visualization, Validation, Methodology, Investigation, Formal analysis. **Anand Sreeram:** Writing – review & editing, Validation, Investigation. **Zhifei Tan:** Writing – review & editing, Supervision, Resources, Project administration, Methodology.

Declaration of Competing Interest

The authors declare that they have no known competing financial interests or personal relationships that could have appeared to influence the work reported in this paper.

Acknowledgements

The authors sincerely acknowledge fundings from the National Natural Science Foundation of China (52408496), the Natural Science Foundation of Hubei Province (2023AFB245), and the Science and Technology Plan Project of Department of Housing and Urban-Rural Development of Hubei Province (2023177).

Data availability

Data will be made available on request.

References

[1] D.T. Addae, M. Rahman, A. Abed, State of art literature review on the mechanical, functional and long-term performance of cold mix asphalt mixtures, Constr. Build. Mater. 400 (2023) 132759.
[2] B. Zhang, X. Yin, Y. Zhong, Q. Zang, Z. Wang, L. Kong, Z. Zeng, S. Fu, Y. Fu, Performance analysis and viscosity modeling of emulsified cutback composite cold-mixed epoxy asphalt binder, Constr. Build. Mater. 416 (2024) 135171.
[3] X. Xu, Z. Leng, J. Lan, W. Wang, J. Yu, Y. Bai, A. Sreeram, J. Hu, Sustainable practice in pavement engineering through value-added collective recycling of waste plastic and waste tyre rubber, Engineering 7 (6) (2021) 857–867.
[4] C. Yan, J. Xi, C. Ai, Z. Leng, Investigating the unique entropy-elasticity of polymer modified asphalt, Clean. Mater. 11 (2024) 100216.
[5] P. Buczyński, J. Krasowski, Optimisation and composition of the recycled cold mix with a high content of waste materials, Sustainability 16 (22) (2024) 9624.
[6] K.M. Chan, F. Zhou, C. Estakhri, New hot-mix cold-laid mix design method with a superpave gyratory compactor, Constr. Build. Mater. 438 (2024) 137051.
[7] M.R.M. Aliha, M. Zalnezhad, P. Jafari Haghighatpour, Fracture toughness of colored slurry seal at low temperatures and different loading Modes: Comparative study with warm and hot mix asphalt materials, Constr. Build. Mater. 409 (2023) 133786.
[8] Z. Cuaran-Cuaran, M. Castilla-Barbosa, O. Rincón, M. Ocampo-Terreros, Evaluation of the electrochemical interaction in the asphalt emulsion-aggregate system of cold mix asphalt through zeta potential and surface free energy analysis, Int. J. Pavement Eng. 25 (1) (2024) 2361837.
[9] R. Hafezzadeh, F. Autelitano, F. Giuliani, Asphalt-based cold patches for repairing road potholes – An overview, Constr. Build. Mater. 306 (2021) 124870.
[10] R. Hafezzadeh, F. Autelitano, F. Giuliani, Performance-related methods for the characterization of cold mix patching materials used in asphalt pavements maintenance, Case Stud. Constr. Mater. 19 (2023) e02600.
[11] S.S. Dash, U.C. Sahoo, Optimised mix design for cold mix asphalt considering various curing parameters of loose mixture, Road. Mater. Pavement Des. 25 (10) (2024) 2167–2184.
[12] D. Lu, X. Jiang, Z. Tan, B. Yin, Z. Leng, J. Zhong, Enhancing sustainability in pavement Engineering: A-state-of-the-art review of cement asphalt emulsion mixtures, Clean. Mater. (2023) 100204.
[13] C. DeLaFuente-Navarro, P. Lastra-González, I. Indacoechea-Vega, D. Castro-Fresno, Rheological and mechanical evaluation of a novel fast curing cold asphalt concrete made with asphalt emulsion, by-products and magnetic induction, Constr. Build. Mater. 449 (2024) 138549.
[14] X. Xu, A. Sreeram, Z. Leng, J. Yu, R. Li, C. Peng, Challenges and opportunities in the high-quality rejuvenation of unmodified and SBS modified asphalt mixtures: State of the art, J. Clean. Prod. 378 (2022) 134634.
[15] X. Xu, Y. Luo, A. Sreeram, Q. Wu, G. Chen, S. Cheng, Z. Chen, X. Chen, Potential use of recycled concrete aggregate (RCA) for sustainable asphalt pavements of the future: A state-of-the-art review, J. Clean. Prod. 344 (2022) 130893.
[16] W. Dong, F. Ma, Z. Fu, Y. Hou, J. Dai, Z. Zhao, R. Fang, Investigating the properties of a novel organic composite warm mix additive on SBS modified asphalt binder, Constr. Build. Mater. 444 (2024) 137885.
[17] H.A. Dovom, A. Kargari, A.M. Moghaddam, M. Kazemi, E.H. Fini, Self-healing cold mix asphalt containing steel slag: a sustainable approach to cleaner production, J. Clean. Prod. 482 (2024) 144170.
[18] X. Xu, Y. Chu, Y. Luo, Y. Peng, N. Yang, J. Yan, X. Chen, F. Zou, A. Sreeram, Thermal-and-mechanochemical recycling of waste polypropylene into maleated-epoxided degradation products as warm-mix asphalt modifier: Performance improvement and production mechanism analysis, J. Clean. Prod. 426 (2023) 139222.
[19] N. Li, P. Hao, Y. Yao, C. Zhang, The implementation of balanced mix design in asphalt materials: A review, Constr. Build. Mater. 402 (2023) 132919.
[20] H. Wei, Y. Wang, J. Li, Y. Zhang, G. Qian, Optimization design of cold patching asphalt liquid based on performance experiments and statistical methods, Constr. Build. Mater. 391 (2023) 131881.
[21] S.S. Dash, A.K. Chandrappa, U.C. Sahoo, Design and performance of cold mix asphalt–a review, Constr. Build. Mater. 315 (2022) 125687.
[22] D. Benavides, T. López-Montero, M.B. Bizinotto, D. Aponte, Experimental study of asphalt mixtures with recycled resources: Influence of electric arc furnace slag aggregate roughness and bitumen film thickness on fatigue performance, Clean. Mater. 14 (2024) 100282.
[23] P. Meena, G. Ransinchung, P. Kumar, A comparative study on life cycle analysis of cold mix and foamed mix asphalt, IOP Conference Series: Earth and Environmental Science, IOP Publishing, 2024, p. 012093.
[24] K.R. Usman, M.R. Hainin, M.K.I. Mohd Satar, M.N. Mohd Warid, S.N.N. Kamarudin, S. Abdulrahman, Palm oil fuel ash application in cold mix dense-graded bituminous mixture, Constr. Build. Mater. 287 (2021) 123033.
[25] Q. Yang, J. Lin, X. Wang, D. Wang, N. Xie, X. Shi, A review of polymer-modified asphalt binder: Modification mechanisms and mechanical properties, Clean. Mater. (2024) 100255.
[26] R. Li, Z. Leng, Y. Zhang, X. Ma, Preparation and characterization of waterborne epoxy modified bitumen emulsion as a potential high-performance cold binder, Journal of Cleaner Production 235 (2019) 1265–1275.
[27] J. Wang, J. Si, X. Yu, Z. Jiang, M. Zhang, G. Ding, J. Huang, Enhancing the compatibility of cold-mixed epoxy asphalt binder via graphene oxide grafted plant oil-based materials, J. Clean. Prod. 418 (2023) 138209.
[28] X. Wang, Y. Huang, L. Geng, M. Li, H. Han, K. Li, Q. Xu, Y. Ding, T. Zhang, Multiscale performance of composite modified cold patch asphalt mixture for pothole repair, Constr. Build. Mater. 371 (2023) 130729.
[29] H. Wu, M. Yang, W. Song, Z. Wu, D. Chen, X. Chen, Mechanical and rheological properties of polyurethane-polyurea (PU-PUa) modified asphalt binder, Constr. Build. Mater. 411 (2024) 134798.

[30] S. Xu, X. Ren, H. Wu, Z. Zhu, Y. Yang, M. Ling, Design and Water Stability Evaluation of Cold Mix Emulsified Asphalt Mixture under Multiple Freeze-Thaw Cycles, J. Mater. Civ. Eng. 36 (8) (2024).
[31] W. Xu, Y.I. Shah, S. Xu, S. Wang, K. Zhang, X. Fan, B. Liu, Multi-objective optimization of cold mix materials based on response surface methodology, Constr. Build. Mater. 435 (2024) 136782.
[32] F. Kamran, N. Jhora, T.B. Moghaddam, L. Hashemian, Assessment of performance characteristics of pavement base course incorporating reclaimed asphalt pavement and asphaltenes, Can. J. Civ. Eng. 51 (9) (2024) 989–1003.
[33] Y. Mamuye, M.-C. Liao, N.-D. Do, D.-H. Vo, Performance of Cold-Mix Asphalt with Calcined Eggshell Powder–Activated GGBFS Filler, J. Mater. Civ. Eng. 36 (4) (2024) 04024003.
[34] J. Lin, H. Pan, X. Fang, X. Zhu, J. Hong, Materials design and strength development of a novel cold recycled mixture with asphalt emulsion and geopolymer, Int. J. Pavement Eng. 25 (1) (2024) 2415398.
[35] A.S. Reddy, M. Patil, P.H. Dalal, K.K. Iyer, T.N. Dave, Sustainable utilization of landfill mined soil like fraction in subbase layer for asphalt road applications, Clean. Mater. 11 (2024) 100218.
[36] R. Li, Z. Leng, J. Yang, G. Lu, M. Huang, J. Lan, H. Zhang, Y. Bai, Z. Dong, Innovative application of waste polyethylene terephthalate (PET) derived additive as an antistripping agent for asphalt mixture: Experimental investigation and molecular dynamics simulation, Fuel 300 (2021) 121015.
[37] R. Li, Z. Leng, H. Wang, M.N. Partl, H. Yu, Z. Tan, C. Raab, Microstructure characterisation and constitutive modelling of waterborne epoxy resin modified bitumen emulsion, Int. J. Pavement Eng. 23 (14) (2022) 5077–5086.
[38] X. Zhou, Z. Wang, H. Guo, X. Wang, W. Chen, J. Liu, H. Zhang, C. Wan, Property improvement of epoxy emulsified asphalt modified by waterborne polyurethane in consideration of environmental benefits, Case Stud. Constr. Mater. 21 (2024).
[39] C. Zhou, M. Peng, X. Yang, Y. Qi, B. Xu, Study of the Cold Curing Characteristics of Isocyanate-Modified Asphalt, Materials 17 (5) (2024).
[40] B. Yang, J. Jiang, Z. Leng, X. Jiang, Y. Sun, C. Yan, Z. Tan, G. Li, Maintenance mechanisms of rejuvenator-optimized asphalt emulsion in damaged porous asphalt mixture: Morphological, physicochemical, and rheological characterizations, Constr. Build. Mater. 464 (2025) 140185.
[41] B. Zhang, X. Yin, Y. Zhong, X. Li, S. Fu, Y. Fu, M. Ma, Y. Li, Rheological behavior analysis of emulsified cutback composite cold-mixed epoxy asphalt binder based on apparent viscosity, Constr. Build. Mater. 447 (2024) 138023.
[42] Z. Cao, M. Chen, J. Yu, X. Han, Preparation and characterization of active rejuvenated SBS modified bitumen for the sustainable development of high-grade asphalt pavement, J. Clean. Prod. 273 (2020) 123012.
[43] T. Li, N.H.C. Gómez, G. Lu, D. Liang, M. Oeser, Use of Polyurethane Precursor–Based Modifier as an Eco-Friendly Approach to Improve Performance of Asphalt, J. Transp. Eng. Part B Pavements 147 (3) (2021) 04021031.
[44] Q. Zhang, J. Zhou, D. Wu, J. Zheng, L. Zhang, Preparation and performance evaluation of rubber powder-polyurethane composite modified cold patch asphalt and cold patch asphalt mixture, Constr. Build. Mater. 369 (2023) 130473.
[45] A. Bansode, T. Rahman, L. Carias, O. Asafu-Adjaye, S. Adhikari, B.K. Via, R. Farag, M.L. Auad, Hydrothermal Liquefied Bio-Oil from Municipal Sewage Sludge as a Reactive Filler in Polymeric Diphenylmethane Diisocyanate (p-MDI) Wood Adhesives, Sustainability 17 (3) (2025) 1318.
[46] Z. Zhang, S. Wang, G. Lu, Properties of new cold patch asphalt liquid and mixture modified with waterborne epoxy resin, Int. J. Pavement Eng. 21 (13) (2020) 1606–1616.
[47] M.I. Malik, M.S. Mir, B. Mohanty, Application of solid waste materials in cold bitumen emulsion mixtures for cleaner pavement industry: a comprehensive review, Environ. Sci. Pollut. Res. 31 (36) (2024) 48908–48927.
[48] T.A. Tedla, D. Singh, B. Showkat, Effects of air voids on comprehensive laboratory performance of cold mix containing recycled asphalt pavement, Constr. Build. Mater. 368 (2023) 130416.
[49] D. Zhai, Q. Sun, Molecular dynamics and experimental study of the interfacial adhesion mechanism of polyurethane-based repair materials, Constr. Build. Mater. 459 (2025) 139796.
[50] G. Huang, T. Yang, Z. He, L. Yu, H. Xiao, Polyurethane as a modifier for road asphalt: A literature review, Constr. Build. Mater. 356 (2022) 129058.
[51] R. Matsidik, D. Fazzi, A. Seifert, M. Sommer, Naphthalene Diimide and Pyromellitic Diimide Networks as Cathode Materials in Lithium-ion Batteries: on the Instability of Pyromellitic Diimide, Macromol. Rapid Commun. (2025) 2401121.
[52] Y. Li, C. Wang, Z. Wang, B. Zheng, H. Ma, Y. Zhang, Pyrolysis characteristics analysis of cold mix asphalt mixture based on TG-FTIR-GC/MS, J. Anal. Appl. Pyrolysis 177 (2024) 106385.